Validity of ChPT – is $M_\pi = 135\,\mathrm{MeV}$ small enough ?

Stephan Dürr

University of Wuppertal
Jülich Supercomputing Center

thanks to BMW-collaboration and Regensburg

Lattice 2014 – Columbia University – New York

Outline

- ChPT expansion principles
- Warning about finite-volume effects
- Staggered 2-stout results
- Wilson 2-HEX results
- LEC section of FLAG review
- Assorted remarks and Summary

Overview (1): Rationale for ChPT

- Chiral SU(2) Lagrangian

  LO: 2 LECs [F and $B=\Sigma/F^2$ defined via $m_{u,d}\to 0$, often denoted $F^{(2)}, B^{(2)}$]
  NLO: 7 LECs [$\bar{\ell}_{1\ldots7}\equiv\ln(\Lambda^2_{1\ldots7}/[135\mathrm{MeV}]^2)$]
  NNLO: plethora of LECs
  Value $m_{ud}^{\mathrm{phys}}\simeq 3.5\,\mathrm{MeV}$ ($\overline{\mathrm{MS}}$, 2 GeV) small enough for good convergence.
  Phenomenological LECs depend implicitly on m_s^{phys} and heavier flavors.

- Chiral SU(3) Lagrangian

  LO: 2 LECs [F and $B=\Sigma/F^2$ defined via $m_{u,d,s}\to 0$, often denoted $F^{(3)}, B^{(3)}$]
  NLO: 10 LECs [$L^{\mathrm{ren}}_{1\ldots10}(\mu\sim 770\mathrm{MeV})$]
  NNLO: plethora of LECs
  Value $m_s^{\mathrm{phys}}\simeq 95\,\mathrm{MeV}$ ($\overline{\mathrm{MS}}$, 2 GeV) at the edge of applicability window.
  Phenomenological LECs depend implicitly on m_c^{phys} and heavier flavors.

Here f and $F=f/\sqrt{2}$ used in parallel with $f_\pi^{\mathrm{phys}}\simeq 130.4\,\mathrm{MeV}$ or $F_\pi^{\mathrm{phys}}\simeq 92.2\,\mathrm{MeV}$.

$\oplus$ combine different channels $\longleftrightarrow$ $\ominus$ chiral limit implicit

Overview (2): Employing SU(2) versus SU(3) ChPT

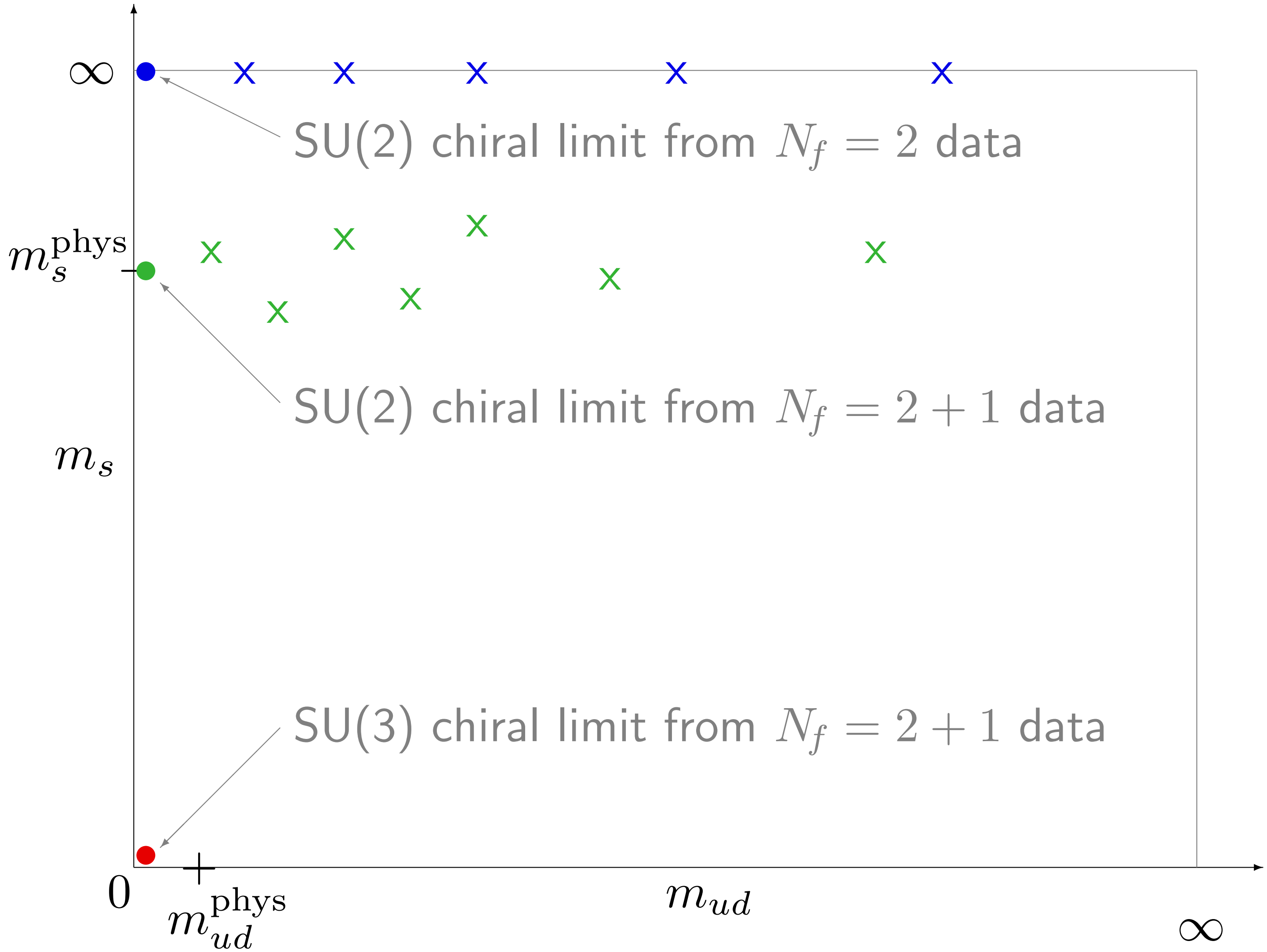

Issues: (i) practical convergence in $m_{u,d}$ or M_π^2, (ii) whether $m_s^{\rm phys}$ still small enough, (iii) potential challenge through $m^{\rm sea} \neq m^{\rm val}$, (iv) potential challenge through $a > 0$.

Overview (3): Expansion in x versus ξ versus X

• plot data versus m_q^{ren}, expand formulas in $x \equiv M^2/(4\pi F)^2$ where $M^2 \equiv B(m_1+m_2)$

$$M_\pi^2 \;=\; M^2 \left\{1+\frac{1}{2}x\ln\frac{M^2}{\Lambda_3^2}+\frac{17}{8}x^2\Big(\ln\frac{M^2}{\Lambda_M^2}\Big)^2+x^2k_M+O(x^3)\right\}$$

$$F_\pi \;=\; F \left\{1-x\ln\frac{M^2}{\Lambda_4^2}-\frac{5}{4}x^2\Big(\ln\frac{M^2}{\Lambda_F^2}\Big)^2+x^2k_F+O(x^3)\right\}$$

• plot data versus M_π^2/F_π^2, expand formulas in $\xi \equiv M_\pi^2/(4\pi F_\pi)^2 = M_\pi^2/(8\pi^2 f_\pi^2)$

$$M^2 \;=\; M_\pi^2 \left\{1-\frac{1}{2}\xi\ln\frac{M_\pi^2}{\Lambda_3^2}-\frac{5}{8}\xi^2\Big(\ln\frac{M_\pi^2}{\Omega_M^2}\Big)^2+\xi^2c_M+O(\xi^3)\right\}$$

$$F \;=\; F_\pi \left\{1+\xi\ln\frac{M_\pi^2}{\Lambda_4^2}-\frac{1}{4}\xi^2\Big(\ln\frac{M_\pi^2}{\Omega_F^2}\Big)^2+\xi^2c_F+O(\xi^3)\right\}$$

• plot data versus M_π^2/GeV^2, expand formulas in $X \equiv M_\pi^2/(4\pi F)^2 = M_\pi^2/(8\pi^2 f^2)$

Coefficients in ξ-expansion smaller in abs. mag. than in x-expansion [cf. FLAG-report].

Lattice: 0806.0894 [JLQCD/TWQCD], 0911.5061 [ETMC], 1108.1380 [NPLQCD]

Overview (4): Curvature and chiral logarithms

Usual logs: $M_\pi^2/(4\pi F_\pi)^2 \cdot \log(M_\pi^2/\mu^2)$ and powers thereof, e.g. $M_\pi(m_q), F_\pi(m_q)$
Naked logs: $\log(M_\pi^2/\mu^2)$ and thus *divergent* in chiral limit, e.g. $\langle r^2\rangle_{S,V}$ of pion

Golterman 0912.4042: "In order to confirm the existence of the chiral logarithm in the data, clearly data points *in the region of the curvature of the logarithm* are needed."

Usual logs in combination with analytic terms: $c_0\xi + c_1\xi\log(M_\pi^2/\mu_1^2)$
Appropriate shift $\mu_1 \to \mu_2$ may remove analytic term: $c_1\xi\log(M_\pi^2/\mu_2^2)$

$$f(M^2) = M^2\log(M^2/\Lambda_i^2) \;\longrightarrow\; f'(M^2) = \log(M^2/\Lambda_i^2) + 1 \;\longrightarrow\; f''(M^2) = 1/M^2$$

- Must go sufficiently chiral to discriminate f'' against 0 (with given statistics).

- In principle the scales Λ_i and $\Lambda_{M,F}$ are arbitrary, but since they originate mostly from integrated vector-meson exchanges they are expected to deviate from $\Lambda \sim 1\,\mathrm{GeV}$ by no more than 1 order of magnitude.

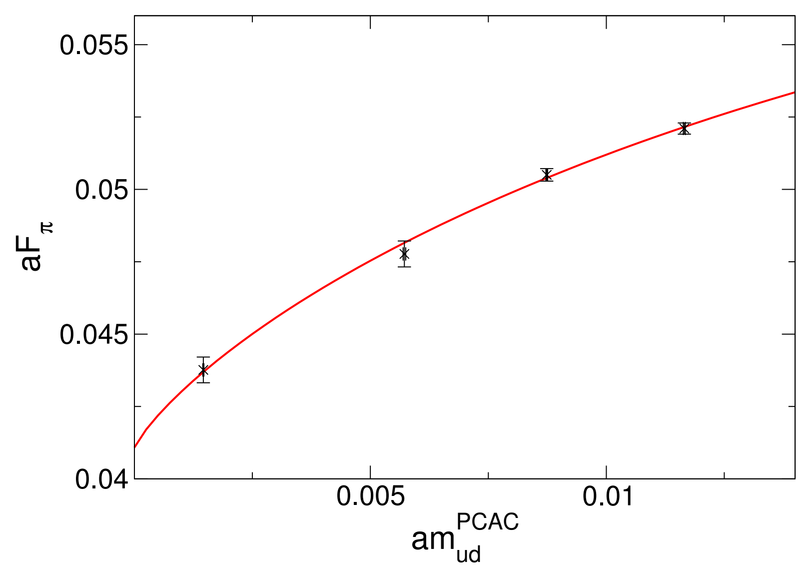

Overview (5): ChPT in finite (euclidean) volume

New scale: spatial box-length L implies $p_{\min} = 2\pi/L$ (with periodic b.c.).
Example: $L = 2\,\mathrm{fm}$ means $p_{\min} \simeq 2\pi\,100\,\mathrm{MeV} \simeq 630\,\mathrm{MeV}$ [edge of applicab. of ChPT].

Finite volume effect on meson masses: $M_\pi(L) > M_\pi \equiv M_\pi(\infty)$.
Finite volume effect on decay constant: $F_\pi(L) < F_\pi \equiv F_\pi(\infty)$.

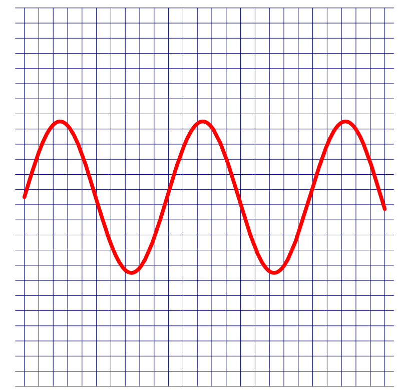

- p-regime: $1 \ll M_\pi L \ll 4\pi F_\pi L$, count $m_q \sim M_\pi^2 \sim p^2 \sim L^{-2}$.
  Box large in absolute units and relative to $M_\pi^{-1} \equiv M_\pi^{-1}(\infty)$.
  Hierarchy of difficulty to access LECs at LO/NLO/NNLO.
- ϵ-regime : $M_\pi L \ll 1 \ll 4\pi F_\pi L$, count $m_q \sim M_\pi^2 \sim \epsilon^4 \sim L^{-4}$.
  Box large in absolute units but small relative to $M_\pi^{-1}(\infty)$, treat U_0 non-perturb.
  Reordering gives preferred access to LO constants $B = \Sigma/F^2$ and F.
- δ-regime : $M_\pi L_s \ll 1 \ll M_\pi L_t \ll 4\pi F_\pi \{L_s, L_t\}$
  Ditto for spatial extent, but not for temporal one [classific. based on $M_\pi \equiv M_\pi(\infty)$].
  Physics of quantum mechanical rotator [Leutwyler, Hasenfratz].

Overview(6): Warning about finite-volume effects

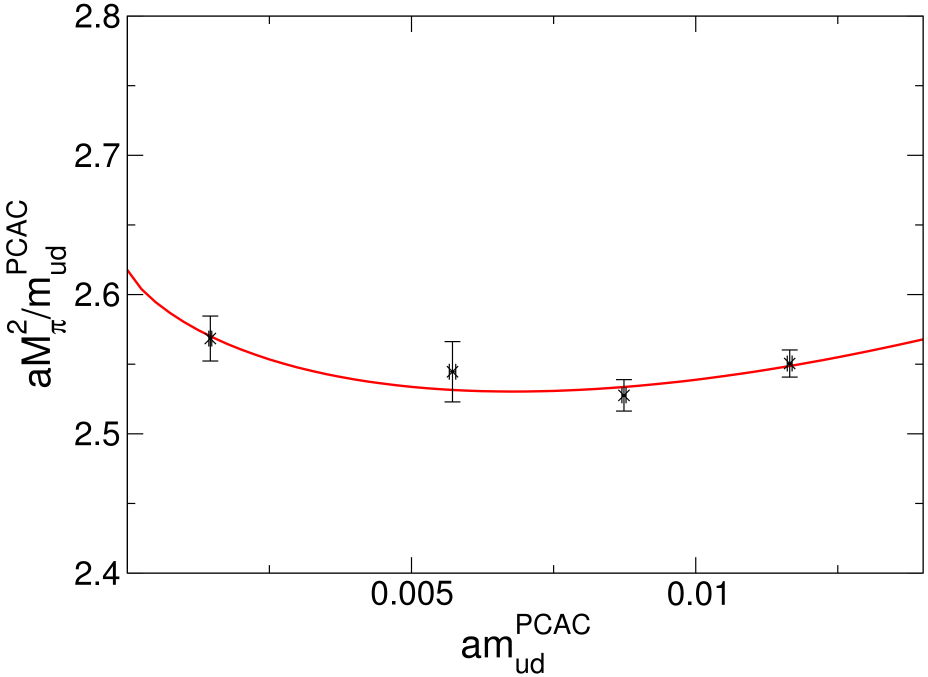

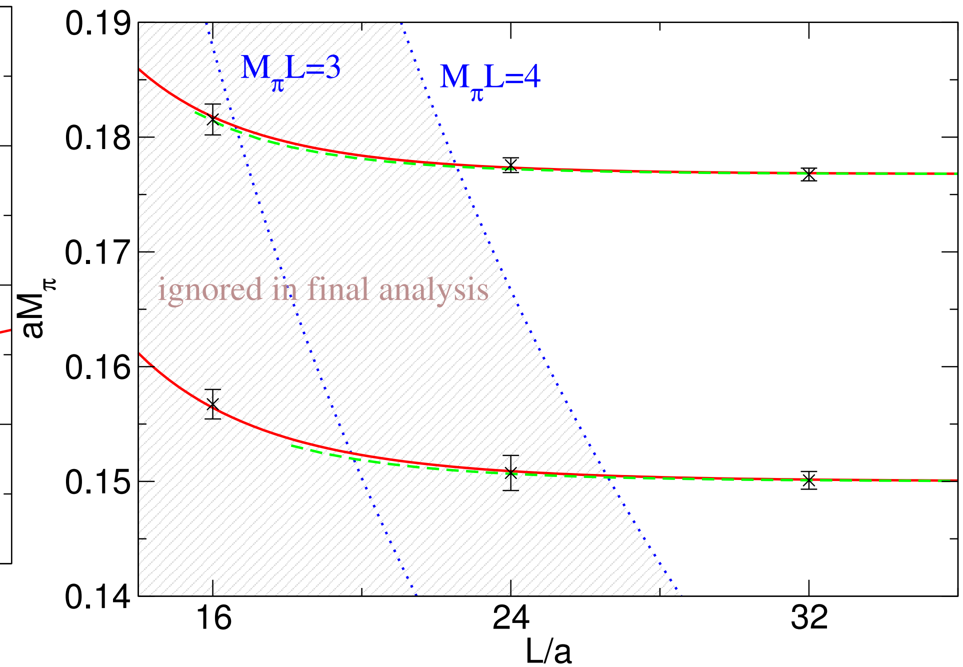

Durr *et al.* [BMW], 1011.2711

$$M_\pi(L) = M_\pi \left\{1 + \frac{1}{2N_f}\xi\tilde{g}_1(M_\pi L) + O(\xi^2)\right\}$$

$$F_\pi(L) = F_\pi \left\{1 - \frac{N_f}{2}\xi\,\tilde{g}_1(M_\pi L) + O(\xi^2)\right\}$$

$$\tilde{g}_1(z) = \frac{24}{z}K_1(z) + \frac{48}{\sqrt{2}z}K_1(\sqrt{2}z) + \ldots \qquad K_1(z) = \sqrt{\frac{\pi}{2z}}\,e^{-z}\left\{1 + \frac{3}{8z} - \ldots\right\}$$

$\Longrightarrow$ In fixed volume L^3 finite-volume effects will lift up $M_\pi^2(m_q)$ and push down $F_\pi(m_q)$ most prominently at small m_q, which may mimic/enhance chiral logs.

Staggered paper (1): Simulation landscape and scale setting

Borsanyi *et al.* [Wuppertal-Regensburg], arXiv:1205.0788.
"SU(2) ChPT low-energy constants from 2+1 flavor staggered lattice simulations"

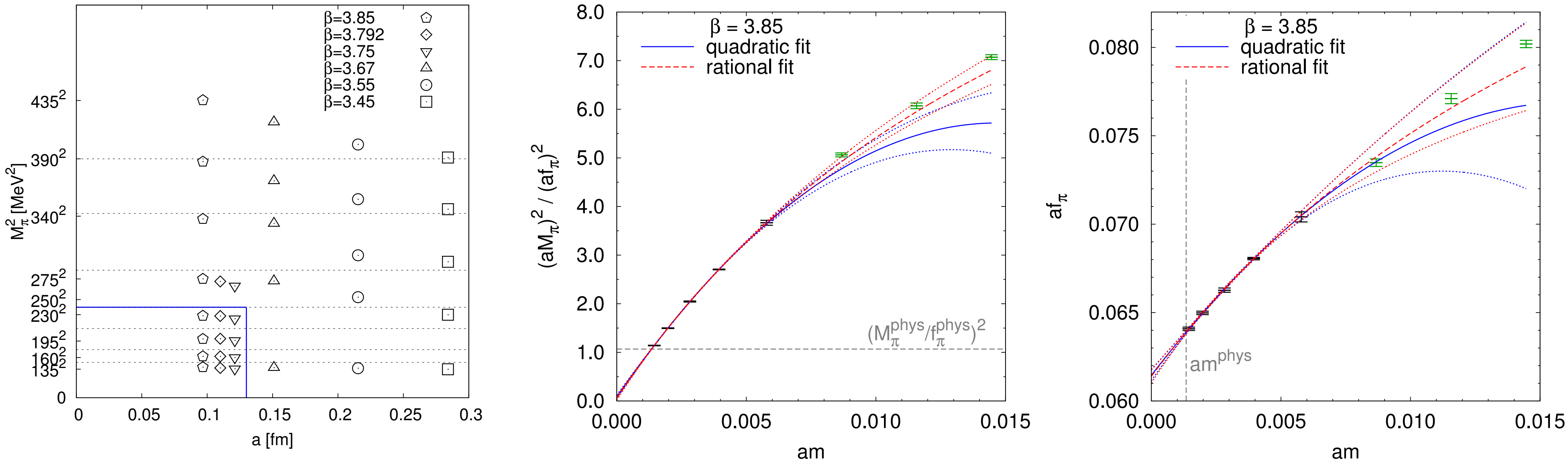

2-stout staggered lattices with $N_f = 2{+}1$ at various $a = a(\beta)$. Only $m_{ud}^{\mathrm{sea}} = m_{ud}^{\mathrm{val}}$ varies, while $m_s^{\mathrm{sea}} = m_s^{\mathrm{val}}$ tuned to m_s^{phys}. Scale set via f_π^{phys}. Measure only taste-pseudoscalar pions, and compensate finite-volume effects via 2-loop (3-loop) ChPT.

For each β: Interpolate/extrapolate M_π^2/f_π^2 to the point where this ratio assumes its physical value 1.06846, then read off $(am)^{\mathrm{phys}}$.

For each β: Determine af_π for that $(am)^{\mathrm{phys}}$ and thus a via f_π^{PDG}

Staggered paper (2): Joint SU(2) chiral fit at NLO

$$M_\pi^2 \;=\; (aM_\pi)^2/a^2 \;=\; \chi\left[1+\frac{\chi}{16\pi^2 f^2}\log\frac{\chi}{\Lambda_3^2}\right]$$

$$f_\pi \;=\; (af_\pi)/a \;=\; f\left[1-\frac{\chi}{8\pi^2 f^2}\log\frac{\chi}{\Lambda_4^2}\right],\quad \chi \;=\; 2B\,m \;=\; (2Bm^{\mathrm{phys}})\,\frac{am}{am^{\mathrm{phys}}}$$

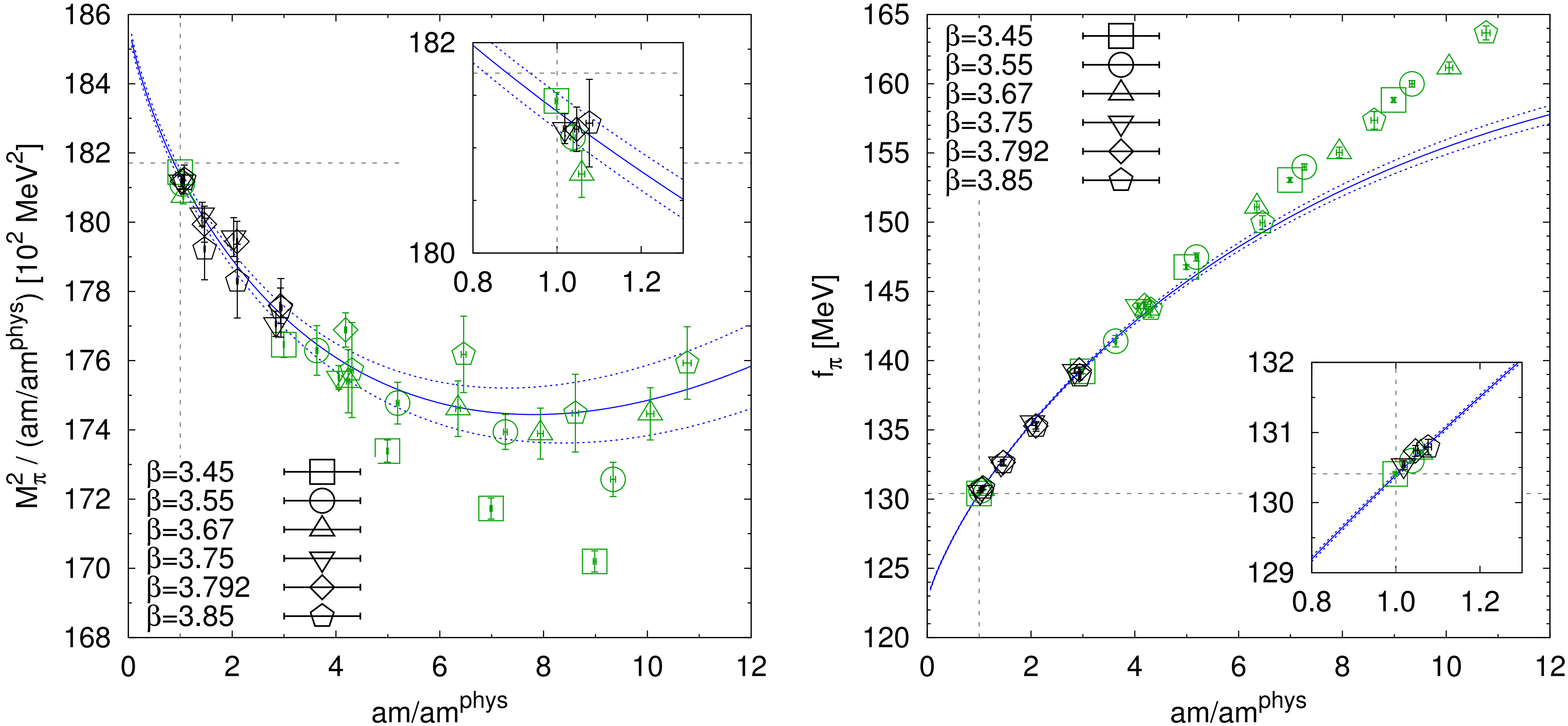

Joint fit to $M_\pi^2 = M_\pi^2(m)$ and $F_\pi = F_\pi(m)$ yields B, F and Λ_3, Λ_4 or $\bar\ell_3, \bar\ell_4$.

Acceptable after restriction to $1.6\,\mathrm{GeV} < a^{-1}$ and $M_\pi \le 240\,\mathrm{MeV}$ (black data).

Staggered paper (3): Sensitivity of LECs on chiral range

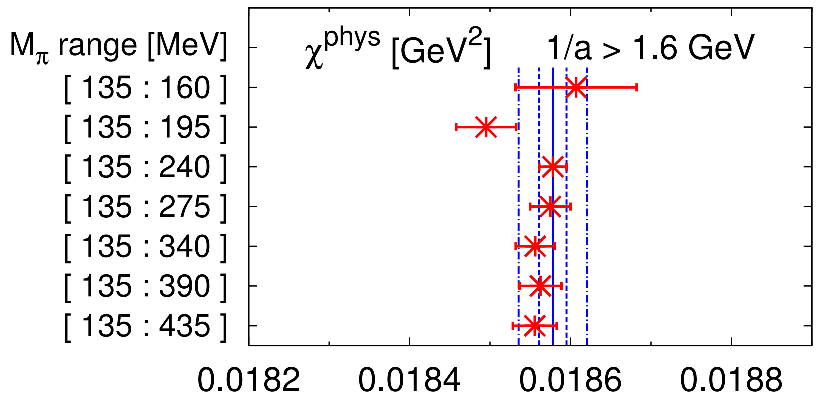

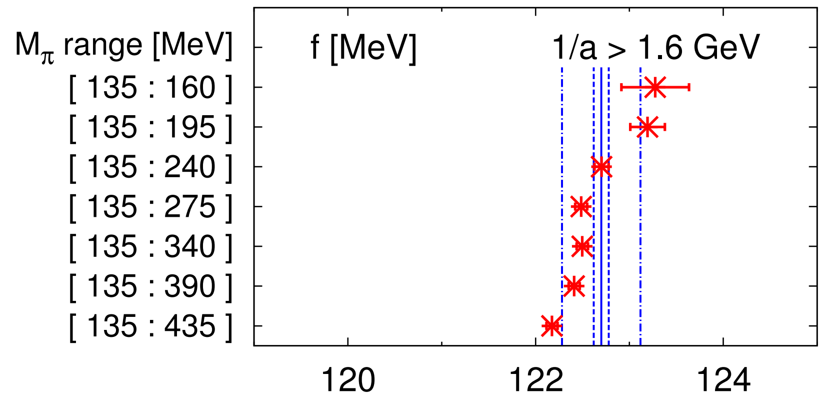

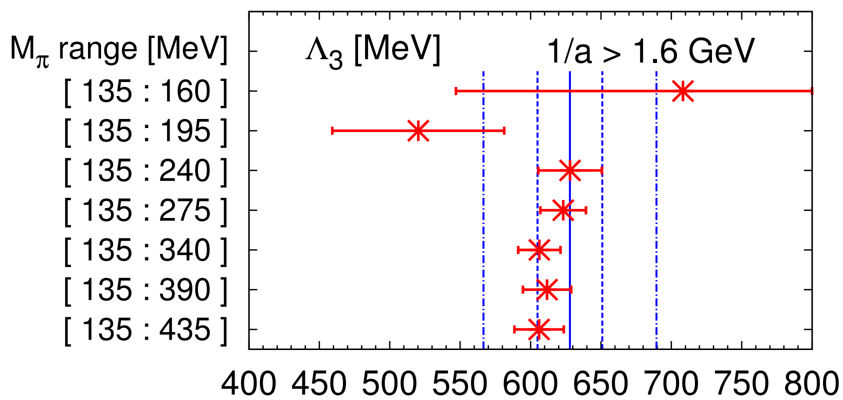

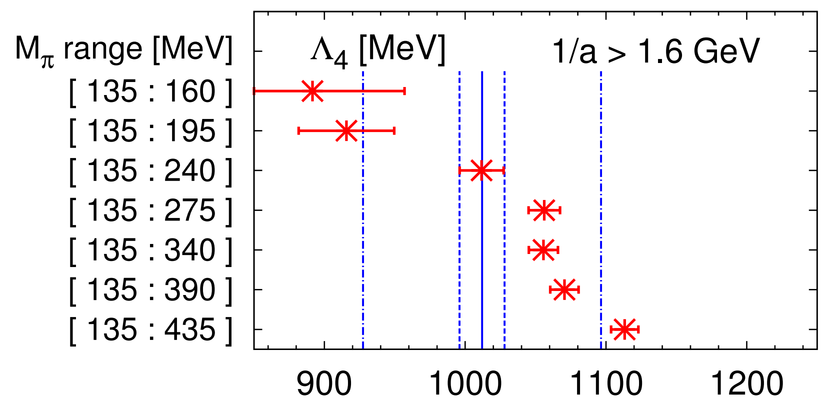

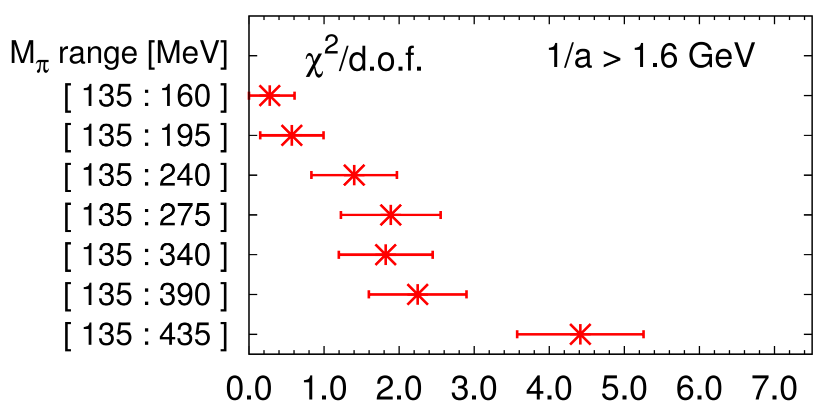

Central value and statistical error from [135:240]MeV fit (with $a^{-1}\!>\!1.6\,\mathrm{GeV}$).

Systematic error from width of distribution ("histogram method").

Staggered paper (4): Sensitivity on cuts from above/below

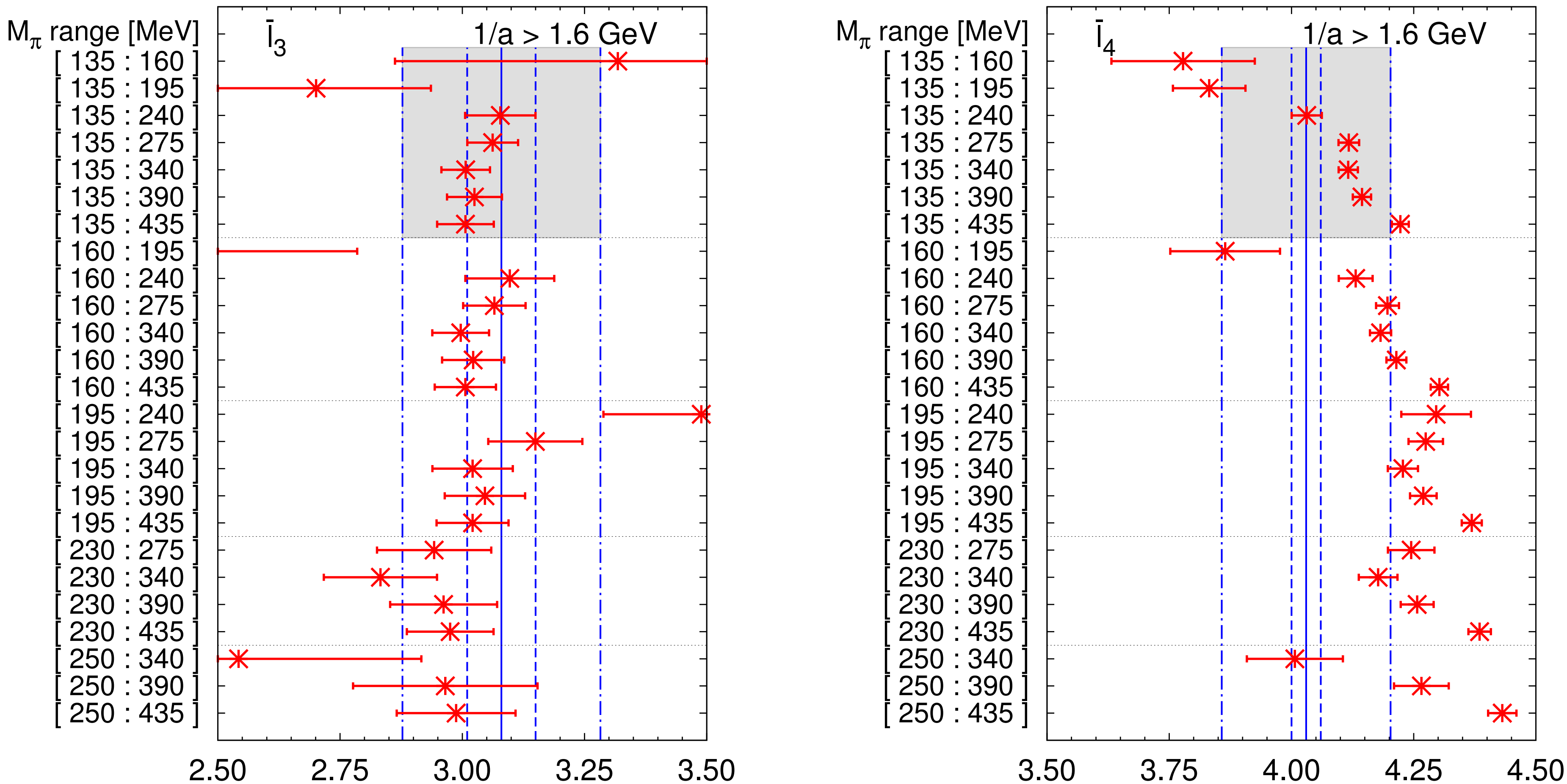

Deliberately leaving out near-physical mass points barely affects results for $\bar{\ell}_3$ (left), but increases instability for $\bar{\ell}_4$ (right).

Staggered paper (5): Breakup into LO/NLO/NNLO parts

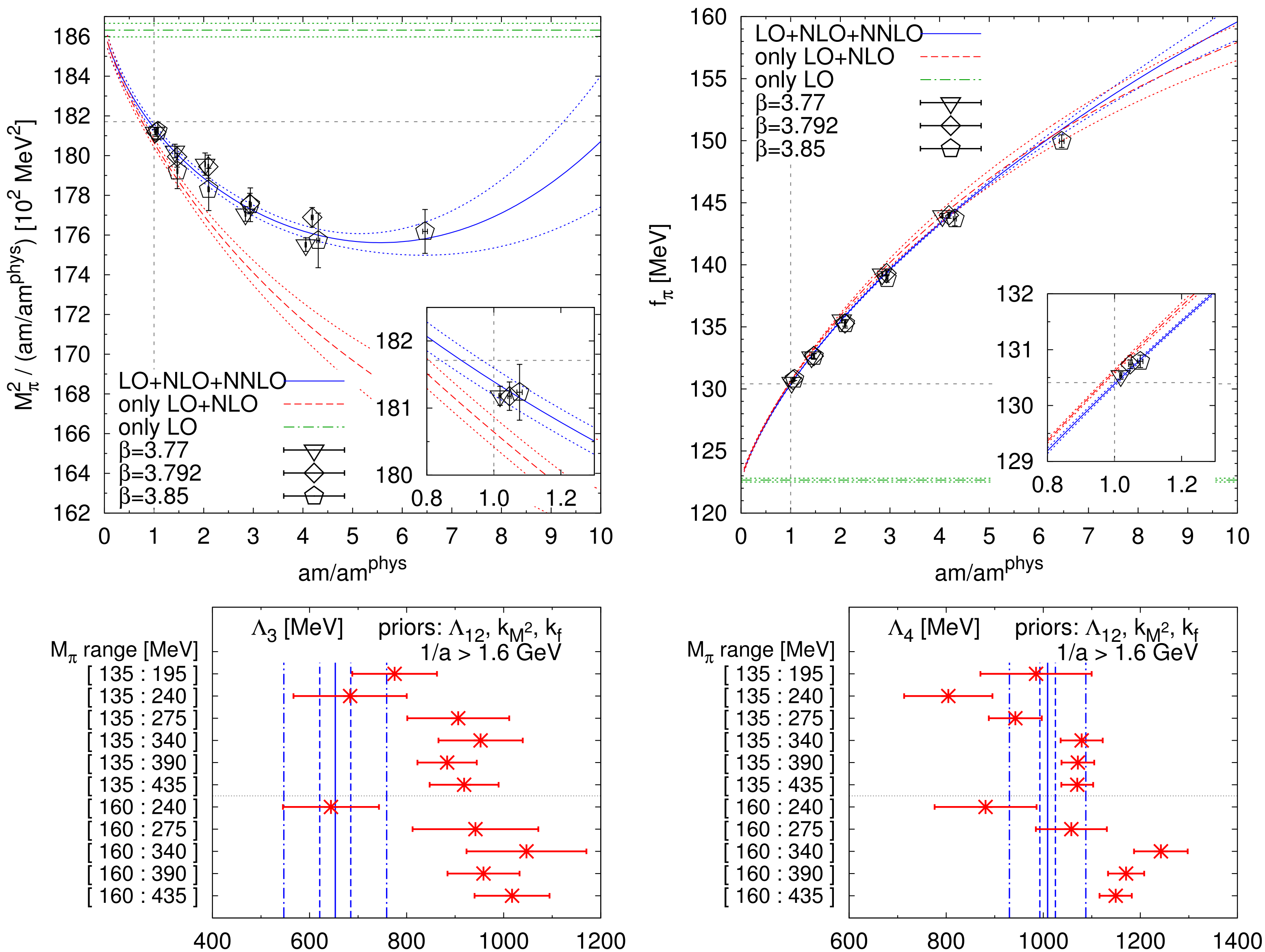

Split-up of LO+NLO+NNLO fit (priors for NNLO part) suggests good convergence at physical mass point and yields $\Lambda_{3,4}$ consistent with those from LO+NLO fit.

Wilson paper (1): Global fit strategy and scale setting

Durr *et al.* [BMW collab.], arXiv:1310.3626
"Lattice QCD at the physical point meets SU(2) chiral perturbation theory"

2-HEX tree-level-clover lattices with $N_f = 2{+}1$ at various $a = a(\beta)$. Mainly $m_{ud}^{\mathrm{sea}} = m_{ud}^{\mathrm{val}}$ varies, while $m_s^{\mathrm{sea}} = m_s^{\mathrm{val}}$ scatter around m_s^{phys}. Scale set through Ω baryon mass.

Non-perturbative $Z_{A,S}$ via Rome-Southampton to determine F_π and m_q. Analysis via global fits with dedicated parameters to compensate cut-off and finite-volume effects.

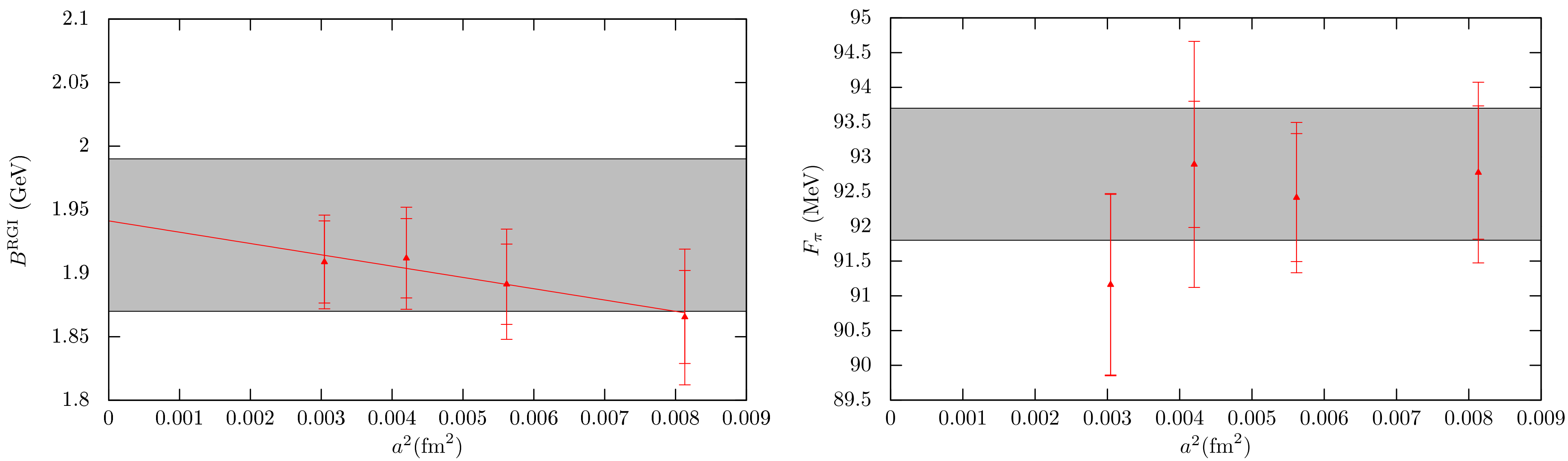

Disentanglement of global fit into per-a values of $B^{\mathrm{RGI}}[\mathrm{GeV}]$ (left) and $F_\pi^{\mathrm{phys}}[\mathrm{MeV}]$ (right) suggest that cut-off effects are mild [left $O(4\%)$, right consistent with 0].

Wilson paper (2): NLO fit via x expansion

Snapshot fit with 4 lattice spacings and $M_\pi \leq 300\,\mathrm{MeV}$:

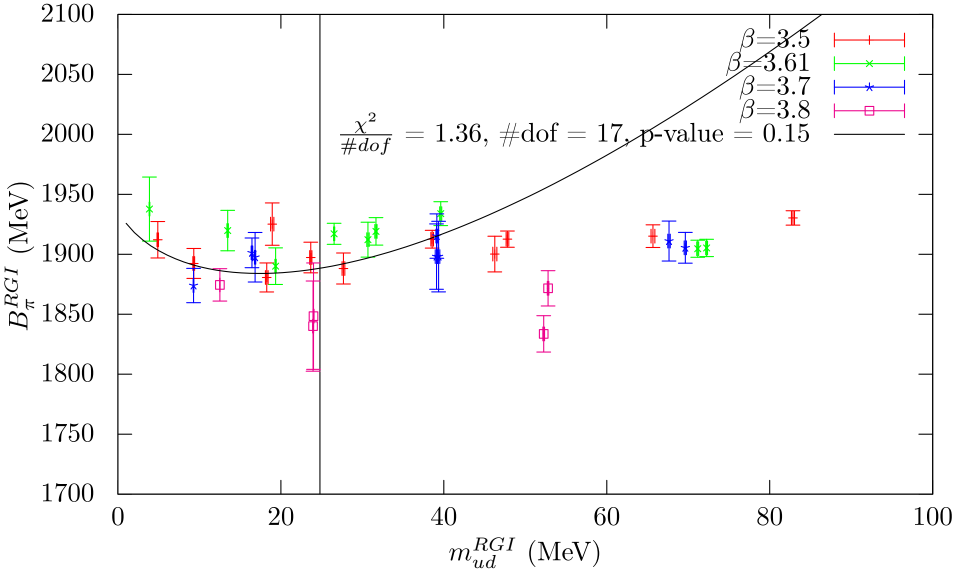

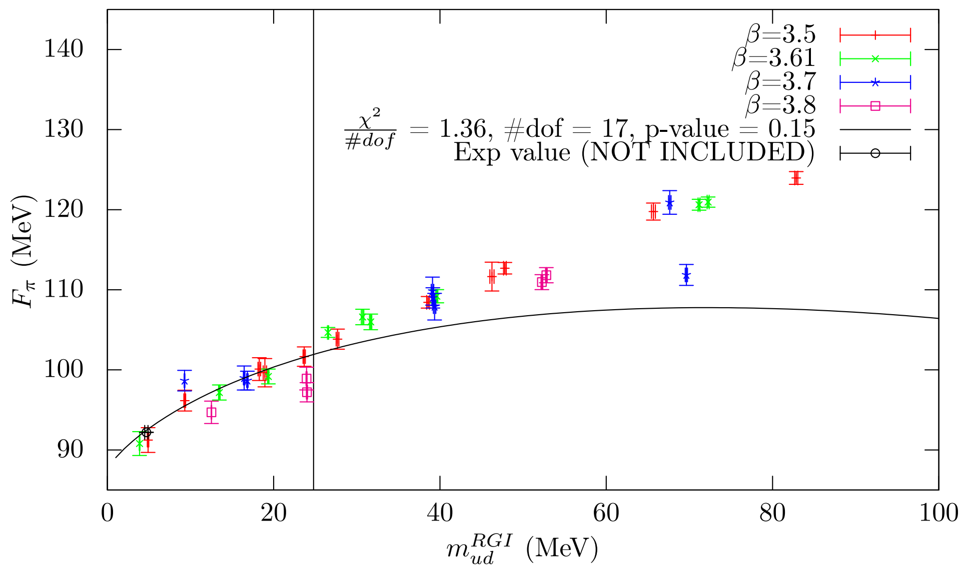

Choice of $M_\pi^{\max}$ affects F more strongly than B:

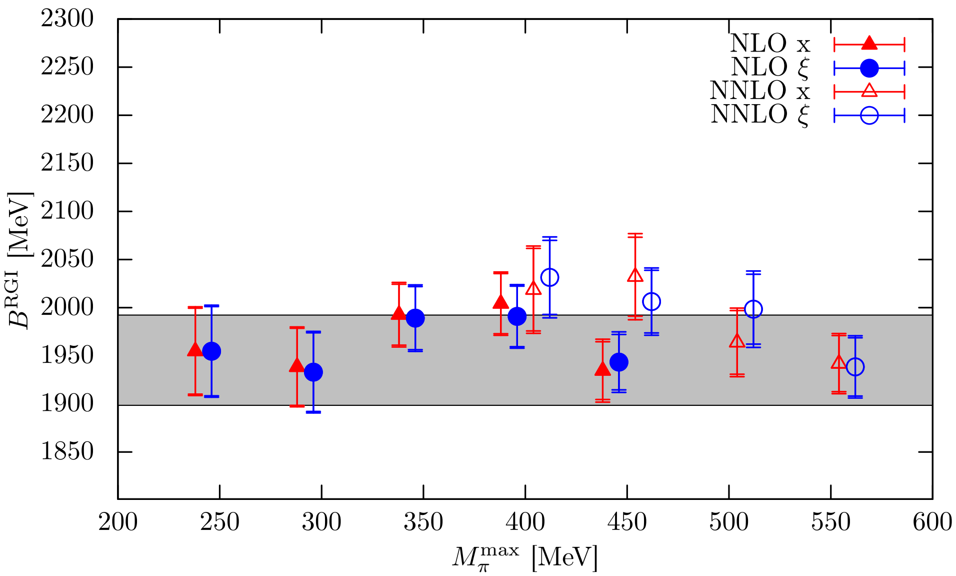

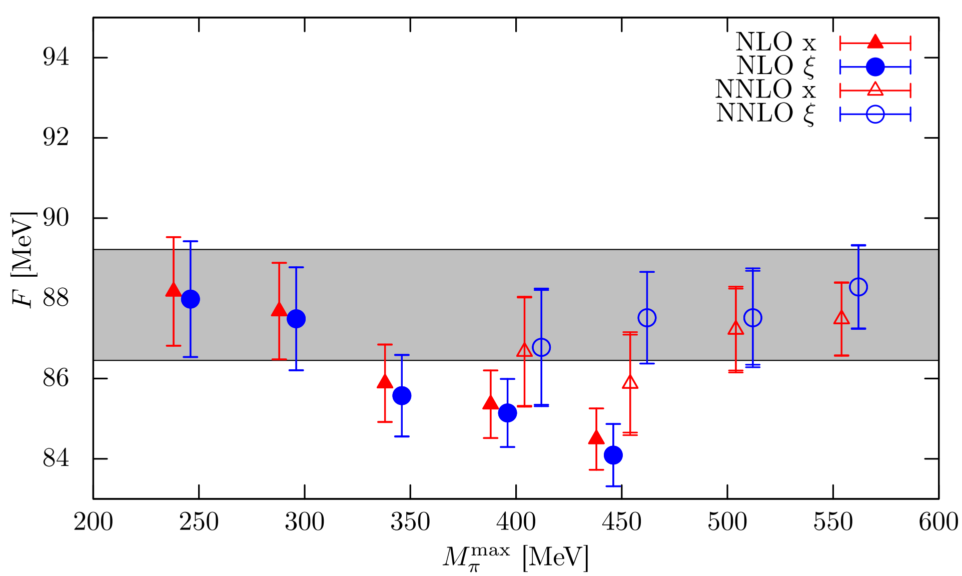

Wilson paper (3): NLO fit via ξ expansion

Snapshot fit with 4 lattice spacings and $M_\pi \le 300\,\mathrm{MeV}$:

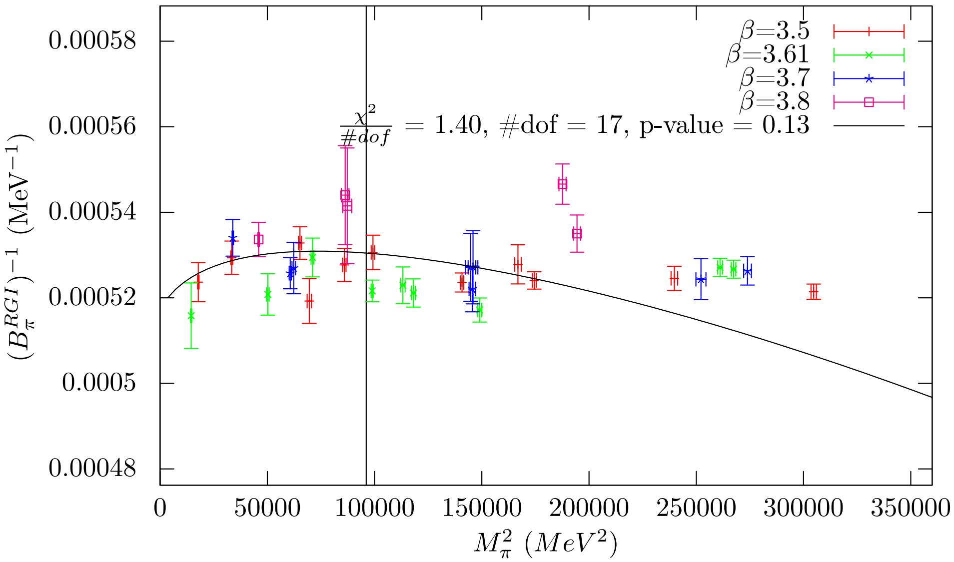

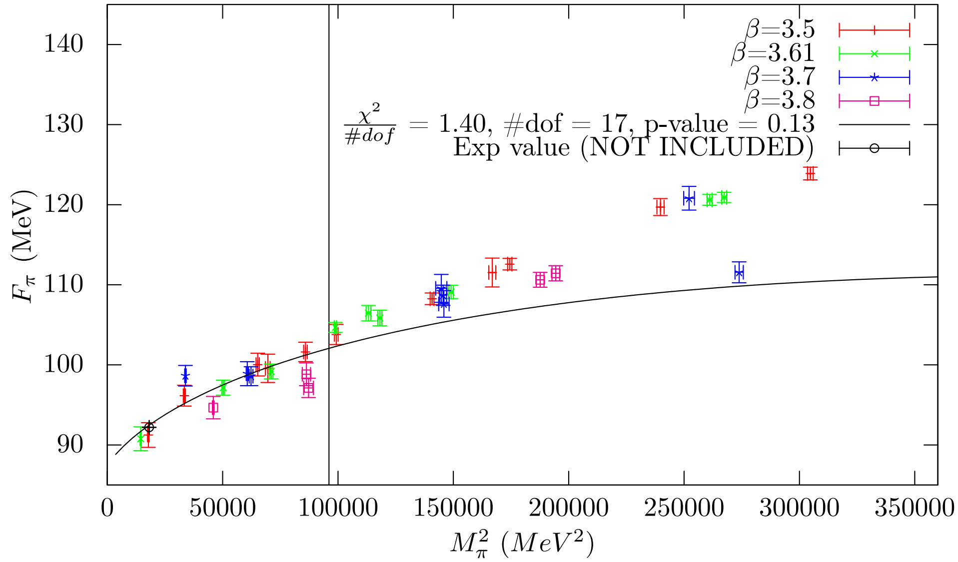

Choice of $M_\pi^{\max}$ affects $\bar{\ell}_4$ more strongly than $\bar{\ell}_3$:

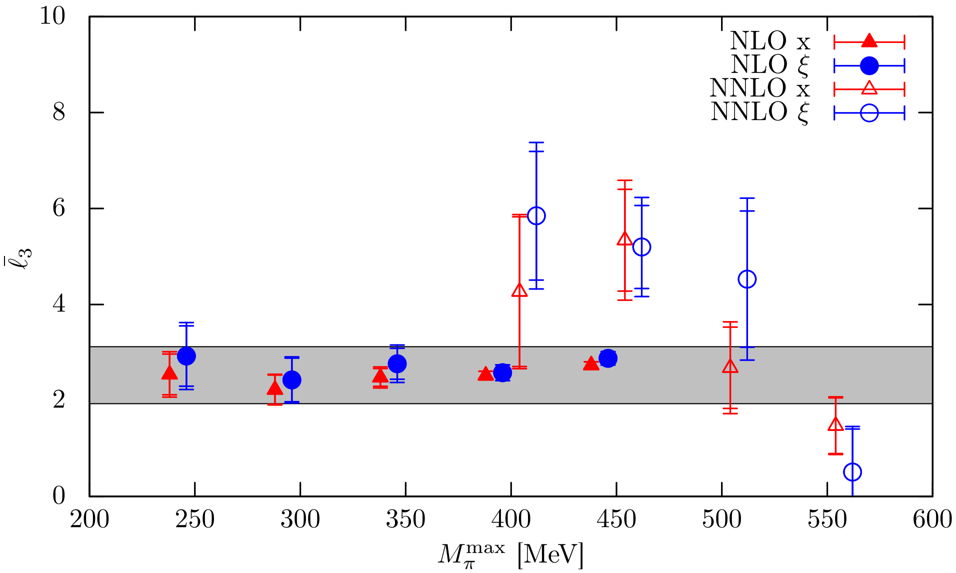

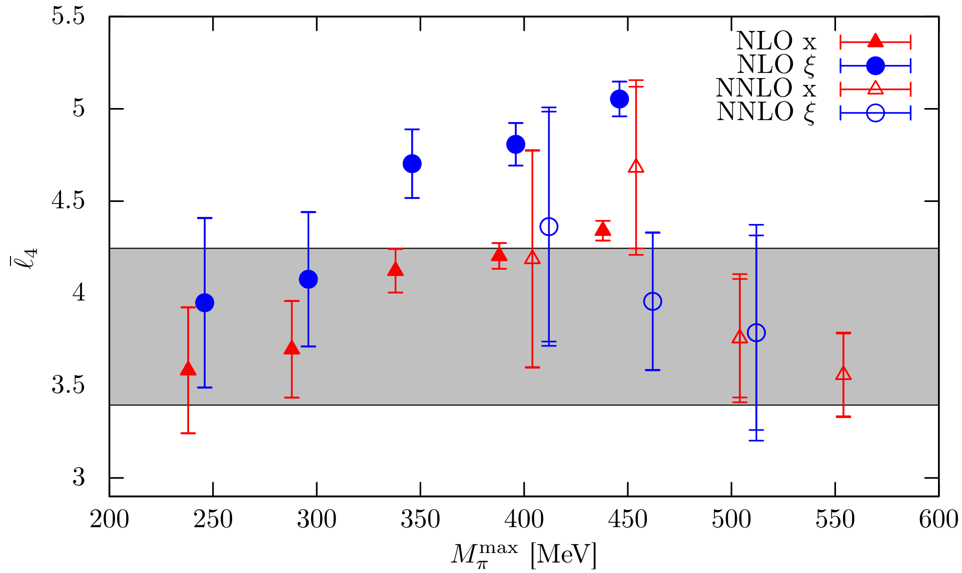

Wilson paper (4): NNLO fit via x expansion

Snapshot fit with 4 lattice spacings and $M_\pi \leq 500\,\mathrm{MeV}$:

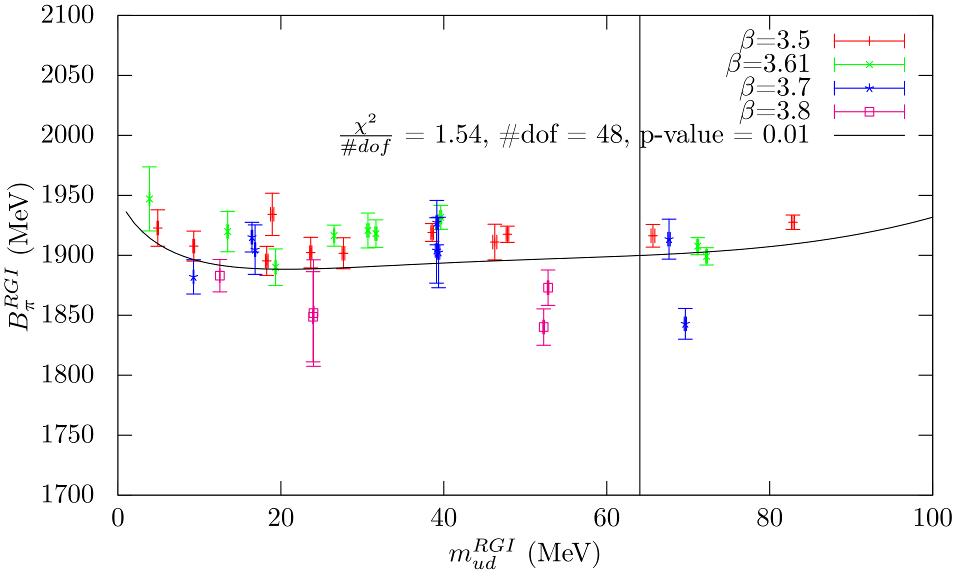

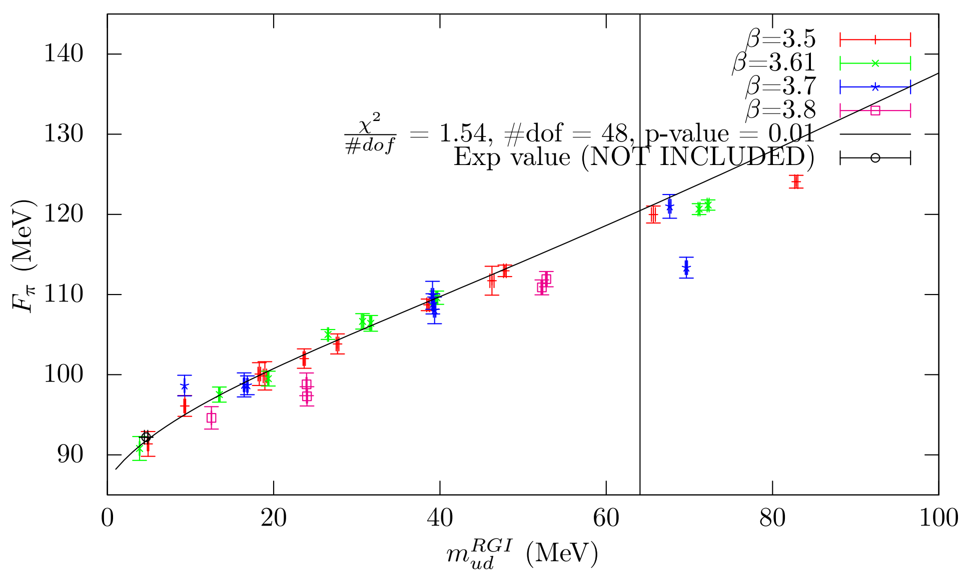

- significantly broader m_{ud} range covered
- curvature tamed for intermediate masses
- smaller p-value than in NLO fit
- NNLO$\ll$NLO$\ll$LO for small enough m_{ud}

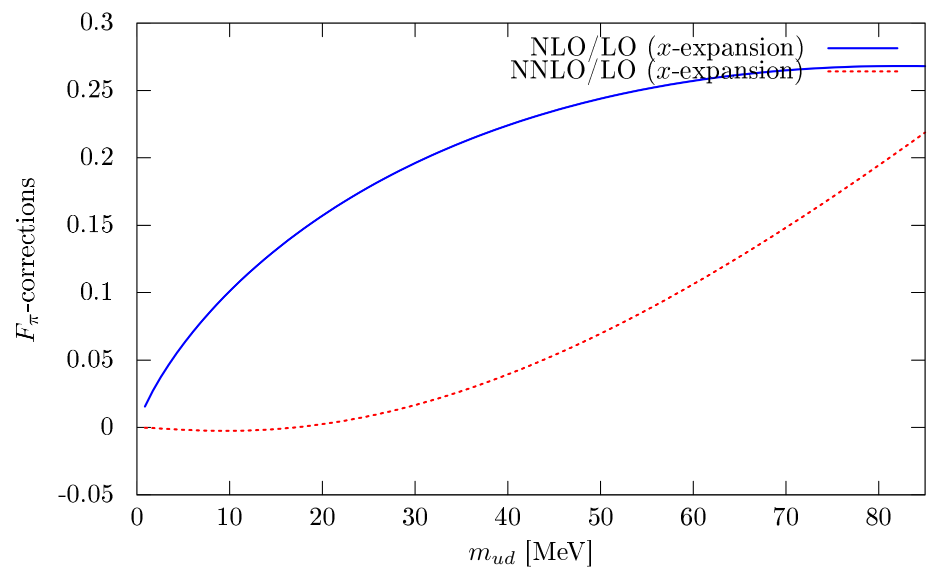

Wilson paper (5): NNLO fit via ξ expansion

Snapshot fit with 4 lattice spacings and $M_\pi \leq 500\,\mathrm{MeV}$:

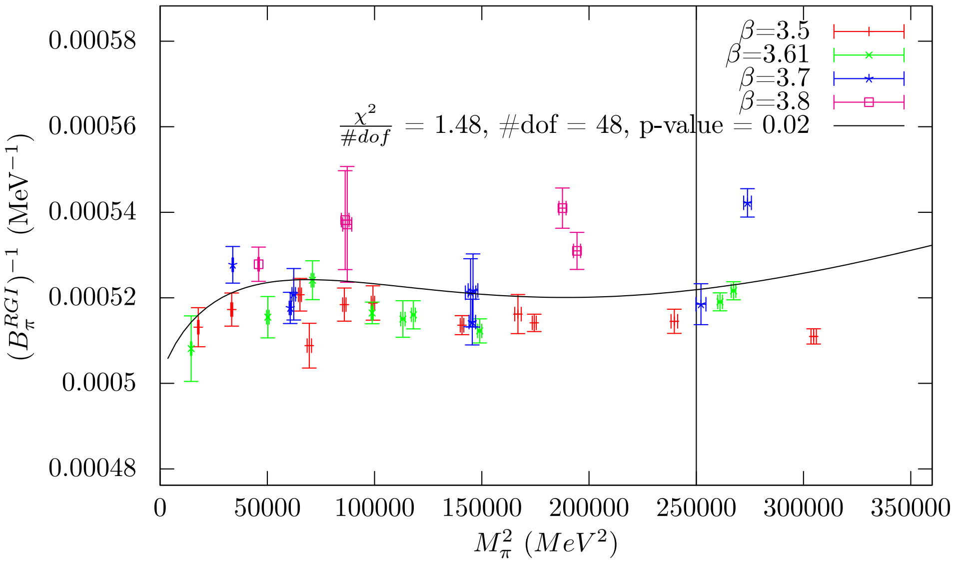

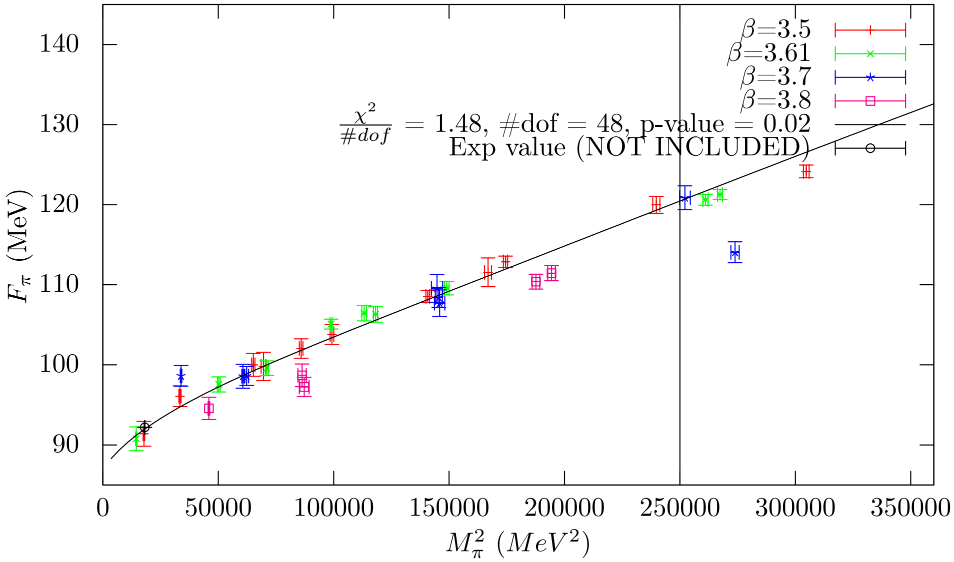

- significantly broader M_π^2 range covered
- curvature tamed for intermediate masses
- smaller p-value than in NLO fit
- NNLO$\ll$NLO$\ll$LO for small enough M_π

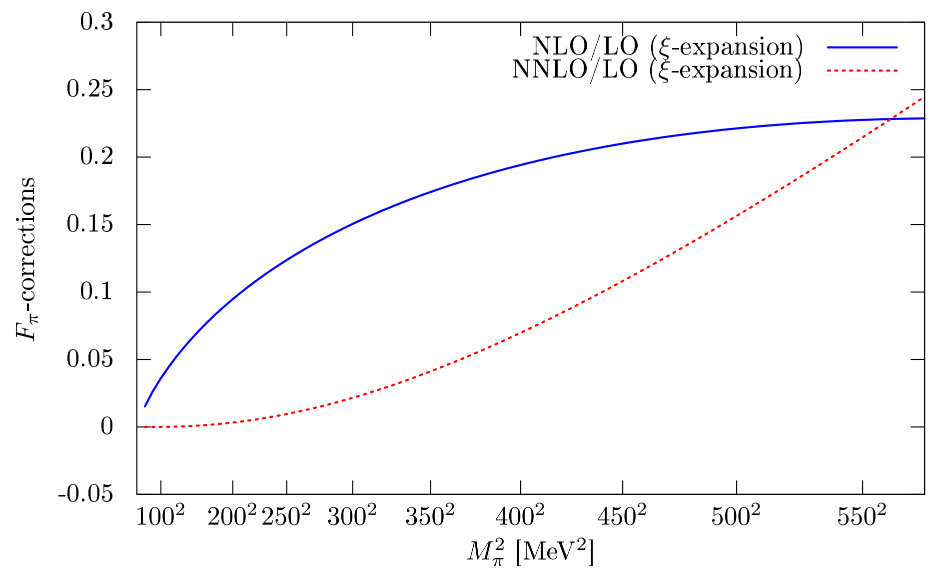

Wilson paper (6): sensitivity on pruning data from below

Choice of $M_\pi^{\min}$ affects F more strongly than B (gray band is final result):

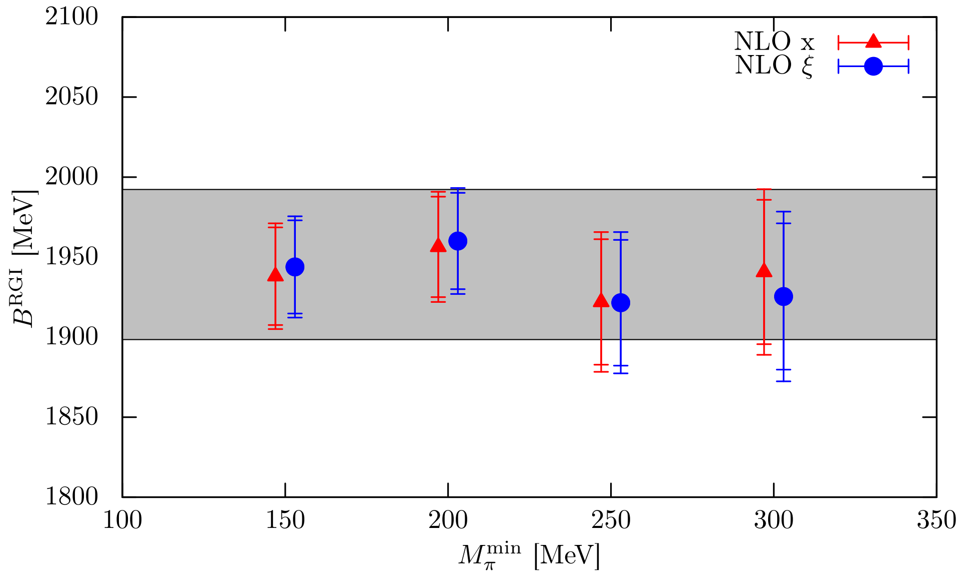

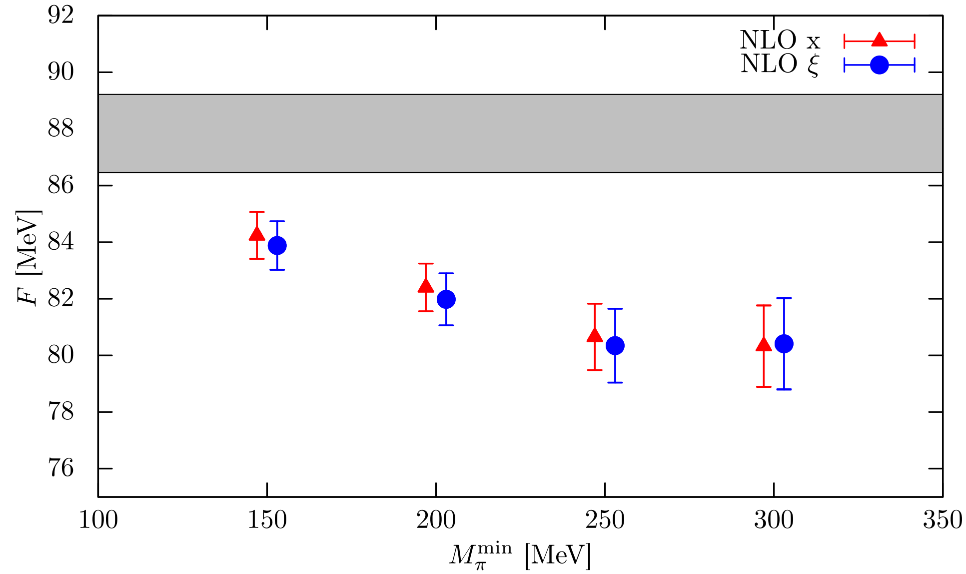

Choice of $M_\pi^{\min}$ affects $\bar{\ell}_4$ more strongly than $\bar{\ell}_3$ (gray band is final result):

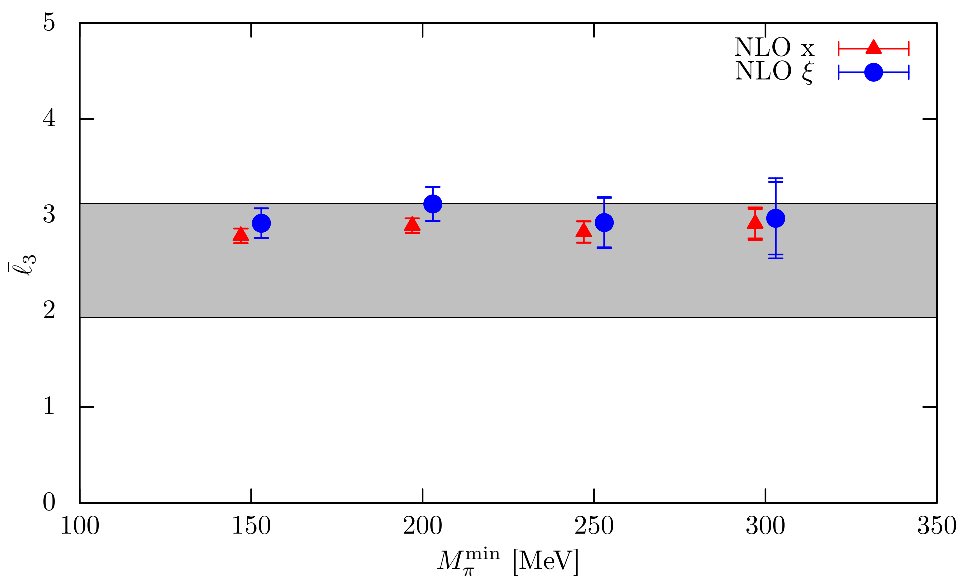

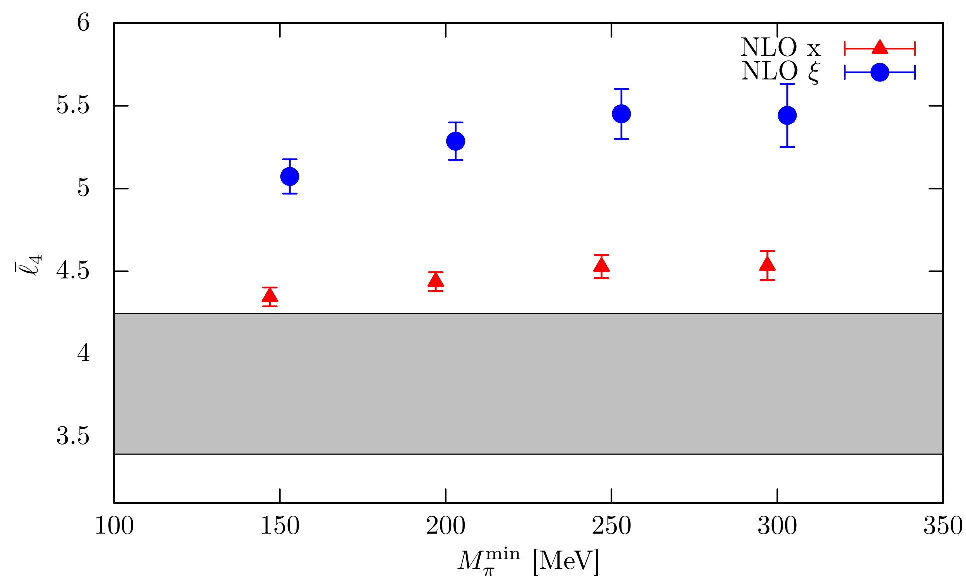

Wilson paper (7): final results

	x-expansion	ξ-expansion
$B_{\mathrm{RGI}}\,[\mathrm{GeV}]$	1.95(04)(01)	1.94(05)(02)
$F\,[\mathrm{MeV}]$	87.9(1.3)(0.3)	87.7(1.4)(0.3)
$\Sigma_{\mathrm{RGI}}^{1/3}\,[\mathrm{MeV}]$	246.9(3.3)(0.9)	246.4(3.5)(1.0)
$\bar{\ell}_3$	2.4(0.4)(0.2)	2.7(0.6)(0.3)
$\bar{\ell}_4$	3.6(0.3)(0.1)	4.0(0.4)(0.1)
$F_\pi^{\mathrm{phys}}\,[\mathrm{MeV}]$	92.7(0.9)(0.2)	92.7(0.9)(0.2)
F_π^{phys}/F	1.054(06)(01)	1.057(07)(01)

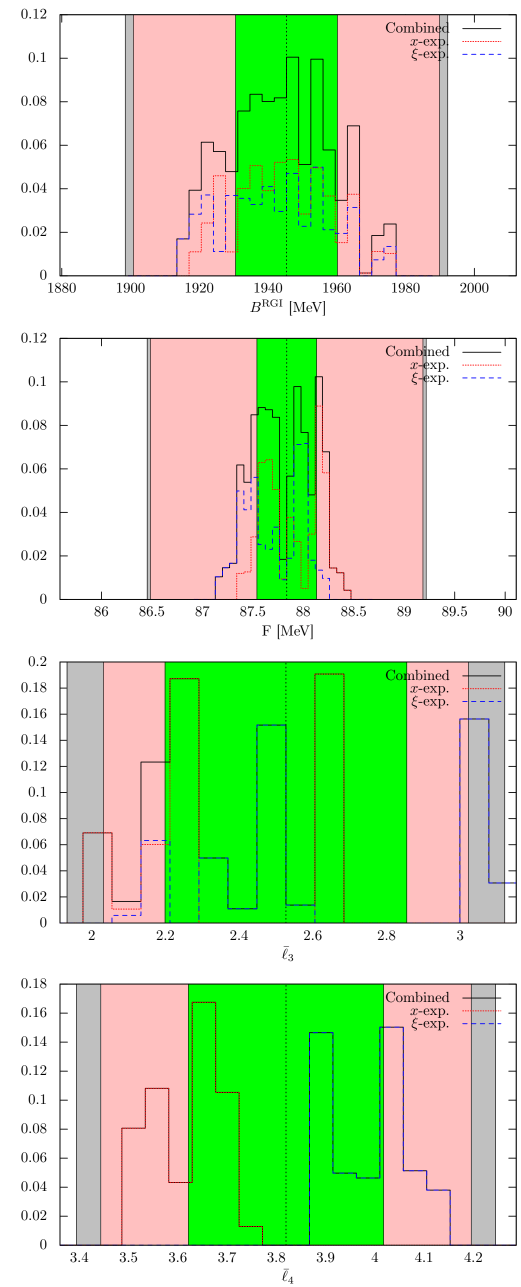

Statistical error determined from 2000 bootstrap samples.

Systematic error determined from width of distribution of legitimate fit results (canonical range $135\mathrm{MeV} \le M_\pi \le 300\mathrm{MeV}$).

- histograms for $B, F, \bar{\ell}_3, \bar{\ell}_4$ from top to bottom
- red/blue histogram for central values in x/ξ-expansion
- reddish/gray bands for statistical/overall error

Flag review (1): summary of $SU(2)$ LECs

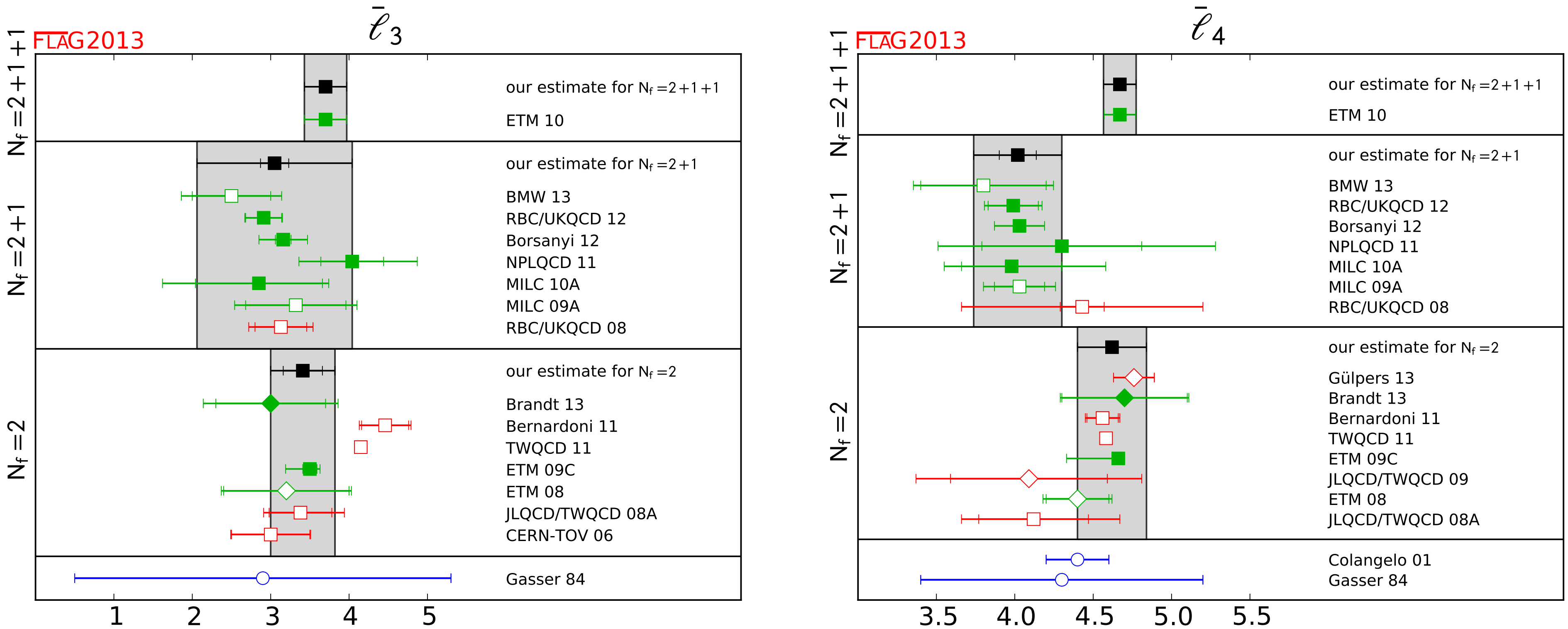

$\bar{\ell}_3$ success: determinations from $N_f=2$, $N_f=2+1$, $N_f=2+1+1$ data overall consistent and more precise than phenomenological determination "Gasser 84".

$\bar{\ell}_4$ more challenging: dependence on N_f in principle possible, but should be monotonic in N_f, phenomenological determination "Colangelo 01" still quite precise.

Flag review (2): summary of $SU(3)$ LECs

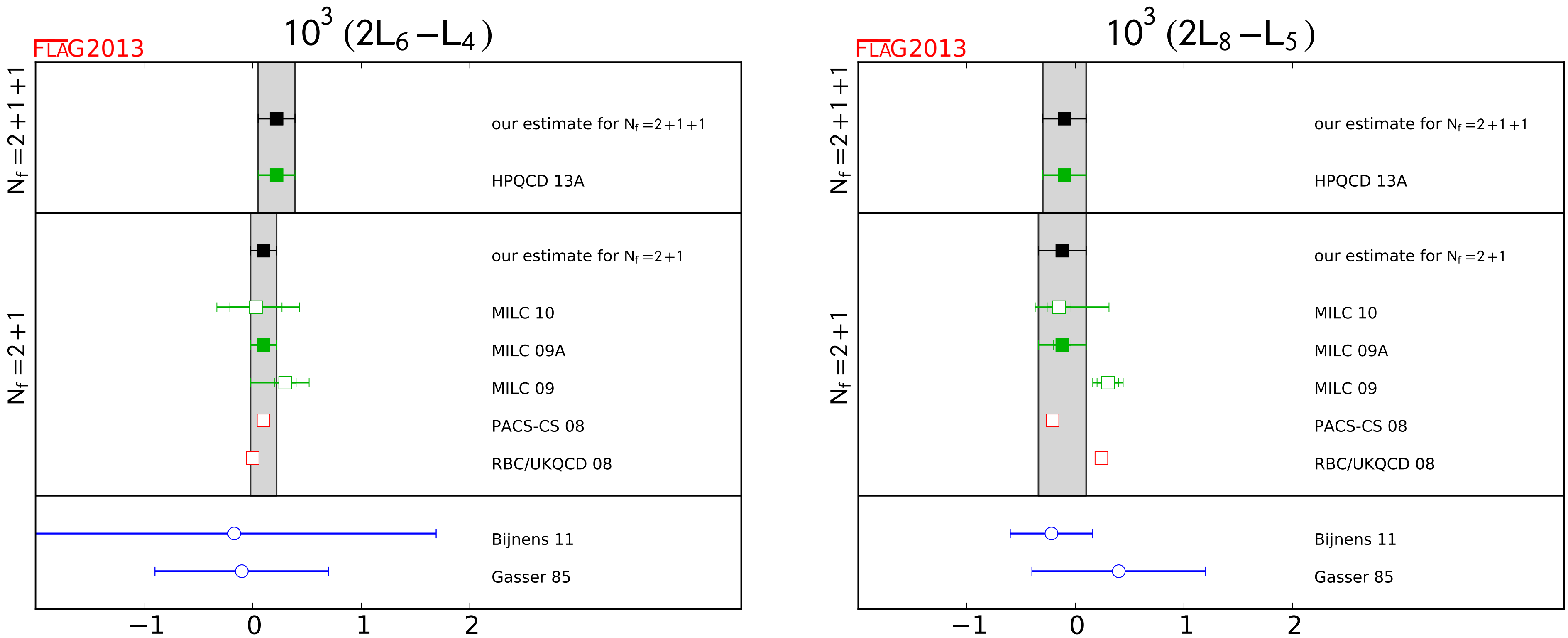

Lattice results available for $L_3, L_4, L_5, L_6, L_8, L_{10}$ and various linear combinations.
In many cases precision significantly better than from phenomenological analyses.

Future: Check $L_{4,6} \stackrel{N_c\to\infty}{\longrightarrow} 0$ and compute $F^{(2)}/F^{(3)}, \Sigma^{(2)}/\Sigma^{(3)}, B^{(2)}/B^{(3)}$ to test Zweig.

Remarks (1): log-free compounds

From the relations given on $x/\xi/X$-expansion transparency one finds

$$M_\pi^4 F_\pi = M^4 F \left\{1 + x \ln \frac{\Lambda_4^2}{\Lambda_3^2} + O(x^2)\right\}$$

- Due to $\gamma_3 = -\frac{1}{2}, \gamma_4 = 2$ the combination $M_\pi^4 F_\pi / m^2$ is linear in m, i.e. log-free up to NNLO corrections; slope yields NLO parameter $\ln(\Lambda_4^2/\Lambda_3^2) = \bar{\ell}_4 - \bar{\ell}_3$.
- In addition, the combination $M_\pi^4 F_\pi$ is free of finite-volume effects through NLO.
- Orthogonal combination $\bar{\ell}_4 + \bar{\ell}_3$ from $M_\pi^4/(F_\pi m^2)$ with pronounced log and FVE.

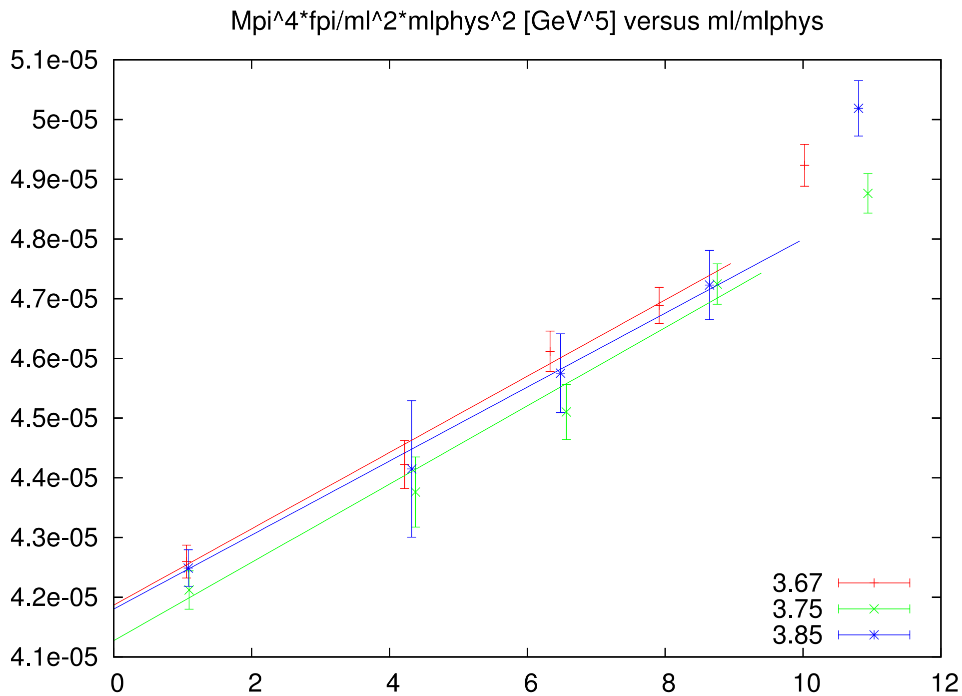

Remarks (2): S-parameter in $N_f = 6, 8, \ldots$ theories

S-parameter decides whether QCD-type theory with $N_f = 6, 8, \ldots$ may explain EW-SB.

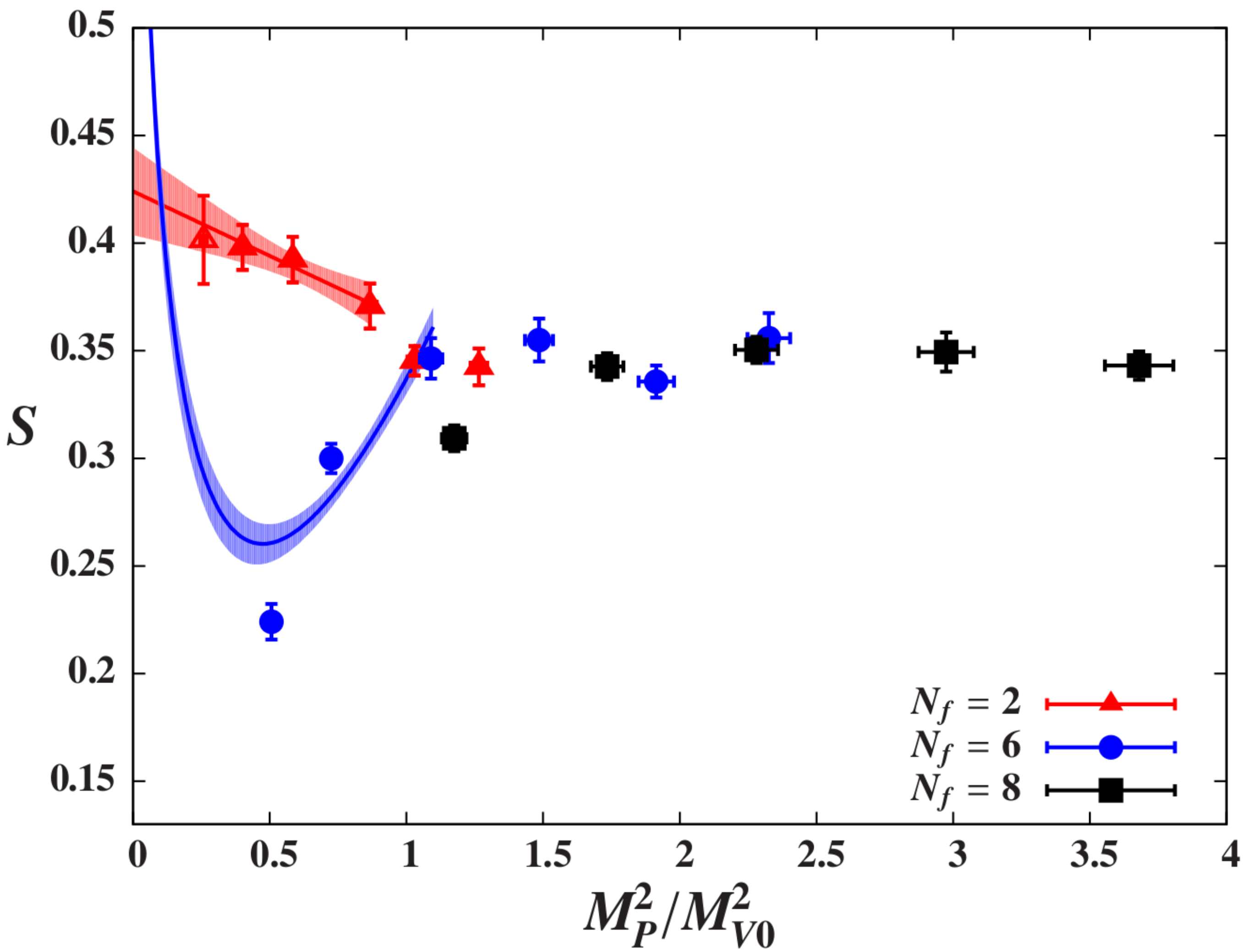

Appelquist *et al.* [LSD coll.], arXiv:1405.4752

- with DW fermions they have $am_{\mathrm{res}} \simeq 0.003$
- real world has $(M_P/M_V)^2 \simeq 0.03$

$\longrightarrow$ Chiral extrapolation under control for $N_f = 2$, issues remain for $N_f = 6, 8, \ldots$.

Summary

- ChPT frameworks exist for 2 or more light quarks, various options for application to $N_f=2$, $N_f=2+1$ and $N_f=2+1+1$ lattice data.

- Beware of finite-volume effects — they mimic/enhance infinite-volume chiral logs.

- ChPT convergence challenged by any one of $\{m, p, 2\pi/L\} \not\ll \Lambda_{\mathrm{QCD}}$, in extended versions also by $m_{\mathrm{sea}} \neq m_{\mathrm{val}}$ and/or $a > 0$. In practice $135\,\mathrm{MeV} \leq M_\pi \leq 400\,\mathrm{MeV}$ seems sufficient to determine mesonic LO and NLO coefficients in most channels.

- Expansion in $\xi \equiv M_\pi^2/(4\pi F_\pi)^2$ in principle better behaved than in $x \equiv 2Bm/(4\pi F)^2$. Sometimes comparing the two at NLO gives a reasonable estimate of NNLO effects.

- Results for QCD look mature; issues remain for EW-SB candidates (S-parameter).

>special thanks to A. Sastre and E.E. Scholz and colleagues from BMW and FLAG<

ChPT talks/posters at this conference

Horkel, Derek: Phase diagram of non-degenerate twisted mass fermions
Nishigaki, Shinsuke: Individual [...] and determination of low-energy constants in two-color QCD+QED
Tiburzi, Brian: Volume effects on the method of extracting form factors at zero momentum
Lytle, Andrew: Hadron spectra and Delta_mix from overlap quarks on a HISQ sea
Murphy, David: The Kaon Semileptonic Form Factor from Domain Wall QCD at the Physical Point

Brown, Nathan: Gradient Flow Analysis on MILC HISQ Ensembles
Hansen, Maxwell: Beyond the Standard Model Kaon Mixing from Mixed-Action Lattice Simulations
Golterman, Maarten: Vacuum alignment and lattice artifacts
Creutz, Michael: Partial quenching and chiral symmetry breaking
Soni, Amarjit: Improved statistics of proton decay matrix element
Leem, Jaehoon: Calculation of BSM Kaon B-parameters using improved staggered quarks in N_f=2+1 QCD
Munster, Gernot: The mass of the adjoint pion in N=1 supersymmetric Yang-Mills theory
Hsieh, Tung-Han: Chiral Properties of Pseudoscalar Meson in Lattice QCD with Domain-Wall Fermion

Kallidonis, Christos: Baryon spectrum with Nf=2+1+1 twisted mass fermions
Aoki, Sinya: Pion masses in 2-flavor QCD with eta-condensation
Gerardin, Antoine: The scalar B meson in the static limit of HQET
Komijani, Javad: Charmed and strange pseudoscalar meson decay constants from HISQ simulations
Neil, Ethan: Leptonic B and D decay constants with 2+1 flavor asqtad fermions
Chang, Chia Cheng: Matrix elements for D-meson mixing from 2+1 lattice QCD

Lujan, Michael: Electric polarizability of neutral hadrons from dynamical lattice QCD ensembles

Bernard, Claude: Finite volume effects and the electromagnetic contributions to kaon and pion masses
Robaina, Daniel: Chiral dynamics in the low-temperature phase of QCD
Du, Daping: B_to_pi semileptonic form factors from unquenched lattice QCD
Kawanai, Taichi: The B_pilnu and Bs_Klnu form factors from 2+1 flavors of domain-wall fermions and relativistic b-quarks